Electronic Supplementary Information

Efficient electroreduction of CO_2 to syngas over ZIF-8 derived oxygen vacancy-rich ZnO nanomaterials

Jie Yang,[a] Hui Wang,[a] Han Yang,[a] Weiwei Dong,*[b] Mingqi Gao,[c] Guangying Zhou,[a] Haiying Tian,[c] Renjie Zhang,[a] Jiqiang Wan,*[c] and Dexin Yang*[a]

[a]*Green Catalysis Center, College of Chemistry, Zhengzhou University, Zhengzhou, Henan 450001, China.*

[b]*Beijing Synchrotron Radiation Facility, Institute of High Energy Physics, Chinese Academy of Sciences, Beijing, 100049, China.*

[c]*Technology Center, China Tobacco Henan Industry Co., Ltd, 450000, Zhengzhou, Henan, China*

*E-mail: yangdx@zzu.edu.cn; dongww@ihep.ac.cn; wanjiqiang1114@163.com

Experimental Section

Chemicals

Zinc nitrate hexahydrate ($Zn(NO_3)_2 \cdot 6H_2O$), 2-methylimidazole, ethanol, and acetonitrile were purchased from Kermel Chemical Reagent Co., Ltd. Acetone was obtained from Sinopharm Chemical Reagent Co., Ltd., P. R. China. Polyethylene oxide-polypropylene oxide-polyethylene (PEO-PPO-PEO, P123) was purchased from Beijing Innochem Technology Co., Ltd. Toray Carbon Paper (TGP-H-60, 19 × 19 cm), tetrabutylammonium bromide (TBAB), Nafion D-521 dispersion (5% w/w in water and 1-propanol), and Nafion N-117 membrane (0.180 mm thick, ≥ 0.90 meg/g exchange capacity) were purchased from Alfa Aesar China Co., Ltd. CO_2 (99.999%) and N_2 (99.99%) were obtained from Henan Yumeng Technology Co., Ltd. 1-Butyl-3-methylimidazolium hexafluorophosphate ([Bmim]PF_6) was supplied by the Centre of Green Chemistry and Catalysis, Lanzhou Institute of Chemical Physics, Chinese Academy of Sciences.

Characterization

The microstructures of ZnO-d and ZnO-n were analyzed by scanning electron microscopy (Care Zeiss SIGMA 500) and transmission electron microscopy (JEOL JEM-2100F) equipped with energy dispersive X-ray spectrometer (EDS). The crystal structures of different ZIF-8 and ZnO were measured by X-ray diffractometer (X'Pert PRO) with the Cu-Kα radiation (λ = 0.15406 nm), the scanning speed was 5^o min^{-1}. The valence states of the elements on ZnO-d and ZnO-n surfaces were investigated by X-ray photoelectron spectroscopy (XPS, Thermo Scientific ESCALab 250Xi) using 200 W Al-Kα source. The base pressure in the analysis chamber was 3×10^{-10} mbar. And the electron binding energies of samples were corrected using the C 1s line at 284.8 eV from adventitious carbon.

Catalysts preparation

Synthesis of ZIF-8 with different morphologies: According to literature reported,[1] 1.05 g of $Zn(NO_3)_2 \cdot 6H_2O$, 1.16 g of 2-methylimidazole, and 3.01 g of TBAB were added to a 100 mL round bottom flask, and the mixture was heated at 60 ºC. After 1 h

stirring, a colorless and transparent solution was obtained. An appropriate amount of H_2O was added into the round bottom flask, and then the transparent solution became turbid. The obtained mixture was separated by centrifugation and the precipitate was washed alternately with H_2O and ethanol for three times. Finally, the product was dried at 60 °C in a vacuum drying oven for 12 h to obtain ZIF-8 nanostructures with dodecahedral morphology (ZIF-8-d). The synthesis procedure of ZIF-8 nanoparticles (ZIF-8-n) is the same with that of ZIF-8-d, except that 3.01g of TBAB was replaced by 0.1 g of P123.

Synthesis of ZnO-d and ZnO-n nanomaterials: The above-mentioned two ZIF-8 nanostructures with different morphologies were ground and annealed at 600 °C for 2 h under air condition. When the temperature naturally cooled down to room temperature, the different ZnO were obtained. The ZnO-d and ZnO-n were derived from ZIF-8-d and ZIF-8-n, respectively.

Electrode preparation: 50 mg of ZnO-d or ZnO-n and 1 mg of carbon black (Vulcan XC 72) were added to a mixed solution of 3 mL of acetone and 30 μL of Nafion D-521 (5 wt%), and the mixture were ultrasonicated for 30 min. After a homogeneous suspension was formed, 0.3 mL of the above suspension was dropped onto a carbon paper substrate (1 × 1 cm^2) and dried at room temperature. The loading mass of ZnO-n or ZnO-d nanomaterials on carbon paper is about 5 mg cm^{-2}.

Electrochemical experiment: The electrochemical experiments were all carried out on the CHI 6081E electrochemical workstation. The LSV scans and electrolysis experiments were performed in a typical H-type cell with a three-electrode system, in which the above-mentioned electrode was used as working electrode, platinum gauze (Pt) was employed as the counter electrode, and Ag/Ag^+ (0.01 M $AgNO_3$ and 0.1 M TBAP in acetonitrile) was used as the reference electrode. In the experiment, a proton exchange membrane (Nafion-117) was used to separate the cathode compartment filled with electrolyte of $[Bmim]PF_6$ (30 wt%)/acetonitrile/H_2O (5 wt%) and anode compartment filled with electrolyte of H_2SO_4 solution (0.5 M). In each experiment, the amount of electrolyte was 25 mL. Before the electrolysis experiment, the catholyte was

purged by CO_2 for about 30 min to form a CO_2-saturated electrolyte. During the electrolysis process, slight magnetic stirring was used under a steady stream of CO_2 (20 sccm) to obtain uniform electrolytes. LSV curves were tested in CO_2- or N_2-saturated [Bmim]PF_6 (30 wt%)/acetonitrile/H_2O (5 wt%) electrolytes over a potential range of −1.0 V to −2.5 V *vs*. Ag/ Ag^+ with a scan rate of 20 mV s^{-1}.

Product analysis: During the electrolysis reaction, gaseous products were analyzed using a gas chromatograph (Agilent 8860) equipped with a thermal conductivity detector (TCD) and a flame ionization detector (FID). In addition, the liquid products were detected using ^1H NMR spectrometer (Bruker Avance III 600 HD) in DMSO-d_6. Then, the FE of different products was calculated according to the corresponding amount of gaseous and liquid products.[2]

EIS measurement: EIS was measured under an open circuit potential condition in [Bmim]PF_6 (30 wt%)/acetonitrile/H_2O (5 wt%) ternary electrolyte with an amplitude of 5 mV and the frequency of 10^{-2}~10^5 Hz.

***C*dl measurement:** The ECSA value is proportional to the value of C_{dl}.[3, 4] The value of C_{dl} was determined by measuring the capacitive current related to double-layer charging from the scan-rate dependence of cyclic voltammogram (CV). The CV scans were measured with various scan rates over a potential range of −1.6 to −1.7 V *vs*. Ag/Ag^+ in a H-type cell. The value of C_{dl} was estimated by plotting the peak current density (*j*) at −1.65 V *vs*. Ag/Ag^+ against the square root of scan rates.

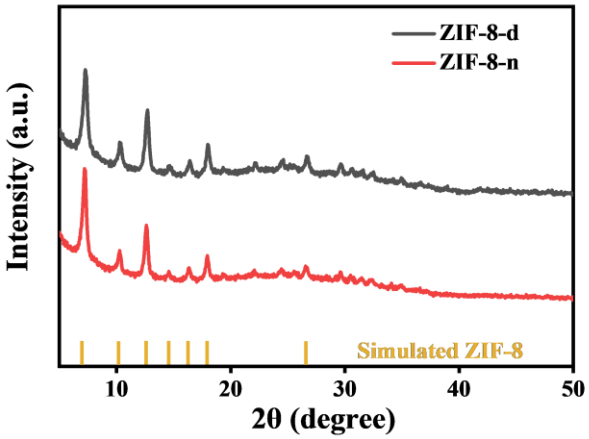

Fig. S1. XRD patterns of ZIF-8-d and ZIF-8-n.

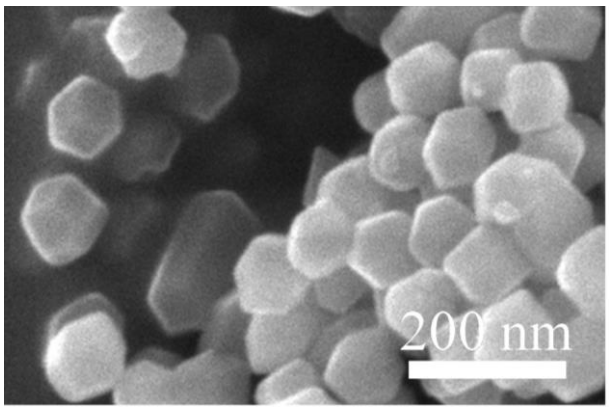

Fig. S2. SEM image of ZIF-8-d.

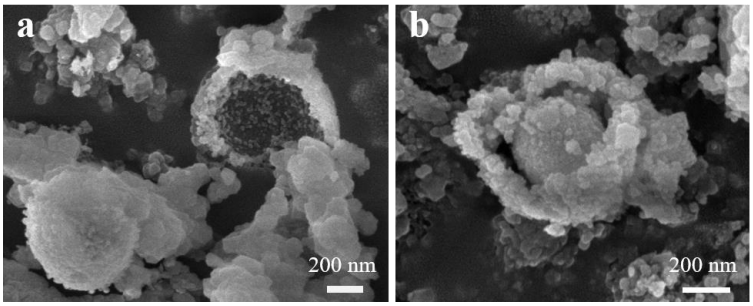

Fig. S3. SEM image of ZIF-8-n.

In Figs. S3a and b, some hollow spheres, spheres, and dispersive nanoparticles are observed in ZIF-8-n, and the homogeneity of ZIF-8-n is poor. Meanwhile, it can observe that these hollow spheres and spheres are made up of many nanoparticles, so we think that the ZIF-8-n is mainly composed of many irregular nanoparticles.

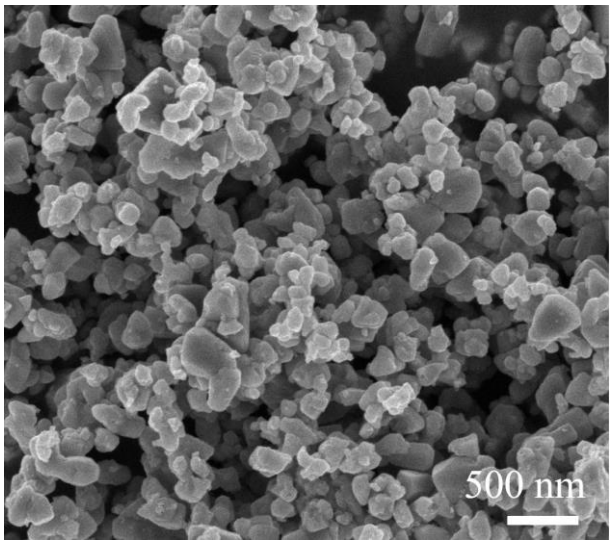

Fig. S4. SEM image of ZnO-d.

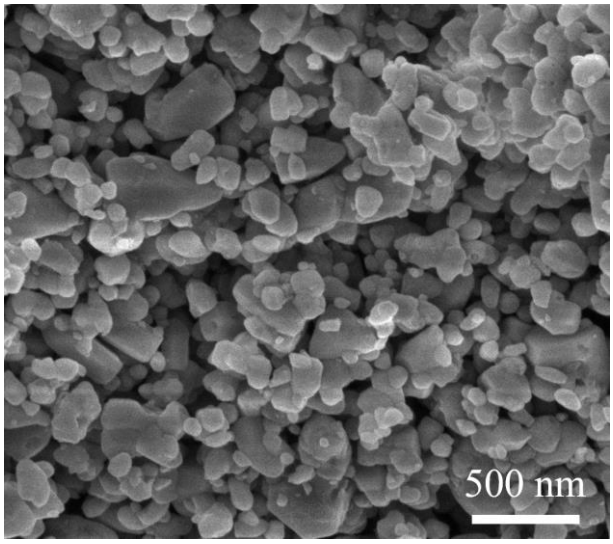

Fig. S5. SEM image of ZnO-n.

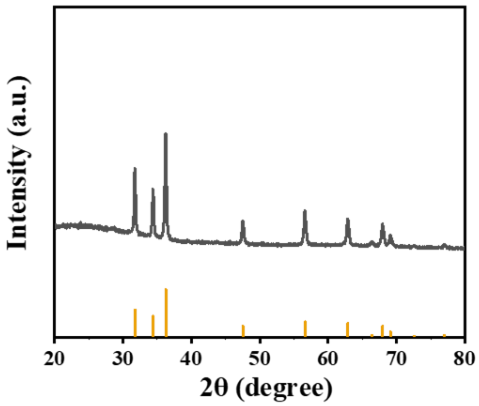

Fig. S6. XRD pattern of ZnO-1.

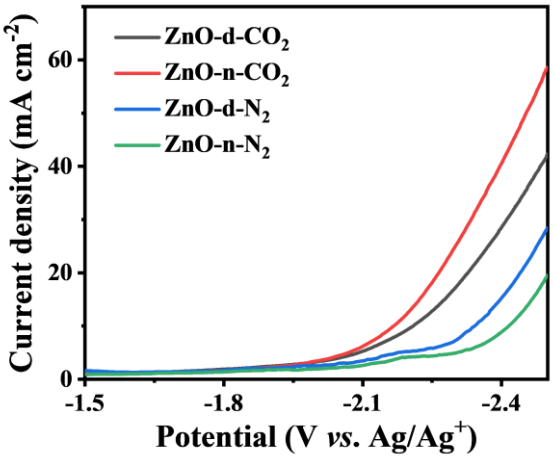

Fig. S7. LSV curves on ZnO-n and ZnO-d in the CO_2- or N_2-saturated [Bmim]PF_6 (30 wt%)/acetonitrile/H_2O (5 wt%) ternary electrolyte.

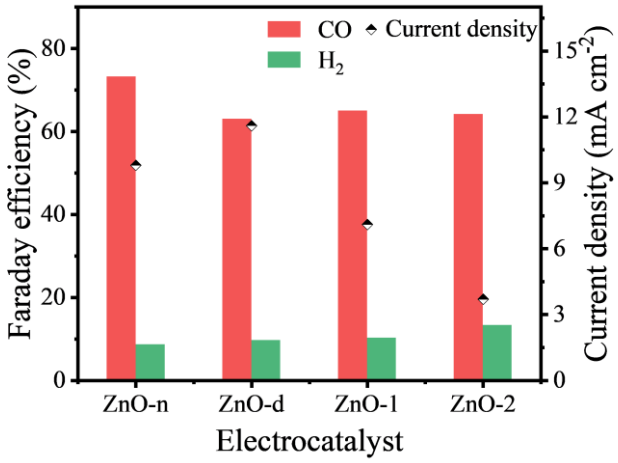

Fig. S8 The current density, maximum CO FE, and H_2 FE over ZnO-n (at −1.9 V vs. Ag/Ag^+), ZnO-d (at −2.1 V vs. Ag/Ag^+), ZnO-1 (at −1.9 V vs. Ag/Ag^+), and ZnO-2 (at −1.9 V vs. Ag/Ag^+).

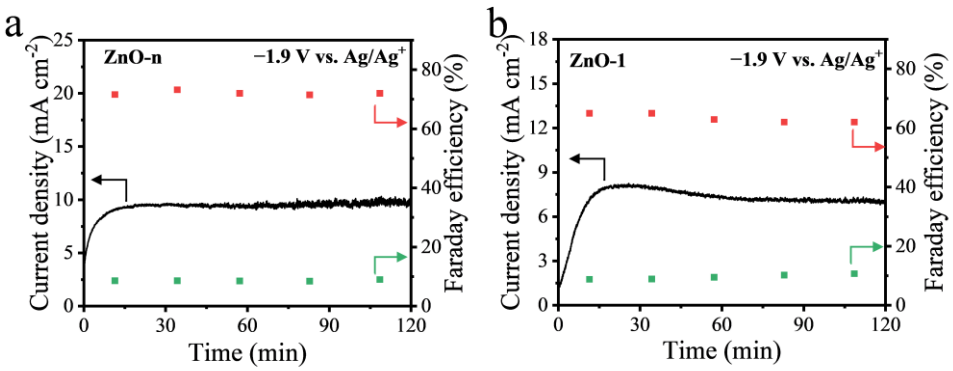

Fig. S9 The i-t curves and FE of CO and H_2 over ZnO-n (a) and ZnO-1 (b).

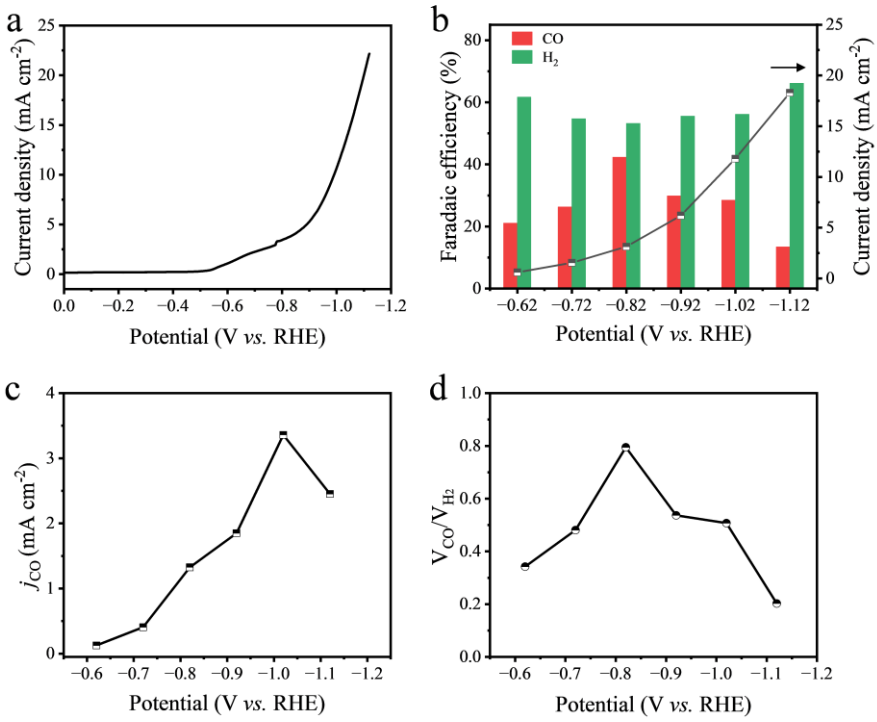

Fig. S10 (a) LSV curve on ZnO-n in the CO_2-saturated 0.5 M $KHCO_3$ electrolyte; (b) FEs of CO, H_2 and current density on ZnO-n at different applied potentials; (c) CO partial current density at different applied potentials for ZnO-n; (d) The volume ratios between CO and H_2 at the applied potentials.

Table S1 Summary of the catalytic performance of Zn-based electrocatalysts for CO_2-to-syngas conversion.

Catalyst	Electrolyte	Potential /V vs. RHE	CO: H_2 ratio	FE_{CO}	Refs
Defective ZnO	0.5 M KOH	−0.6 ~ −1.1 V vs. RHE	~1:7~2:1	50%	[5]
Zn/Cu foam	0.5 M $KHCO_3$	−0.6 ~ −1.3 V vs. RHE	~1:5–2.3:1	40%	[6]
ZnO	0.1 M $KHCO_3$	−0.7 ~ −1.6 V vs. RHE	~1:3.6–2.1:1	~70%	[7]
CuZnO/CNT	0.1 M $KHCO_3$	−0.4 ~ −1.2 V vs. RHE	~1:6.3–1:1	50%	[8]
Zn–Cu alloyed	0.1 M $CsHCO_3$	−0.8 ~ −1.2 V vs. RHE	~1:3.7–5:1	27%	[9]
Zn/Ni	0.1 M KCl	−0.8 ~ −2.4 V vs. RHE	~1.22:1	55%	[10]
$Zn_xCd_{1-x}S$-Amine	0.5 M $NaHCO_3$	−0.76 ~ −1.16 V vs. RHE	~0–19.7:1	~80%	[11]
CuZnAl-Oxide	0.1 M $KHCO_3$	−0.89 ~ −1.89 V vs. RHE	~1:2–1:5	25%	[12]
oxide-derived Zn	0.5 M $KHCO_3$	−0.7 ~ −1.1 V vs. RHE	~1:3.3–1.1:1	55%	[13]
ZnCu	0.5 M $KHCO_3$	−1.0 ~ −1.8 V vs. RHE	~1:4–0.74:1	47.2%	[14]
defective ZnO doped carbon	0.5 M $KHCO_3$	−0.8 ~ −1.3 V vs. RHE	~1:1.5–2.7:1	71%	[15]
Zn film	0.5 M $KHCO_3$	−0.67 ~ −1.27 V vs. RHE	~1:11.1–11.4:1	92.6%	[16]
Zn/ZnO_{NR}	0.1 M $NaHCO_3$	−0.58 ~ −1.38 V vs. RHE	~1:4.5–4:1	62.7%	[17]
ZnO-d, ZnO-n	[Bmim]PF_6 (30 wt%)/acetonitrile /H_2O (5 wt%)	−1.7 ~ −2.2 V vs. Ag/Ag^+	~1:3–8.5:1	73.2%	This Work

Table S2 The effect of [Bmim]PF_6 concentration in the electrolyte for CO_2 electroreduction on ZnO-n at −1.9 V vs. Ag/Ag^+.

[Bmim]PF_6 concentration (wt%)	Current density	FE_{CO}	FE_{H2}	V_{CO}/V_{H2}
20	3.7 mA cm^{-2}	39.4%	44.8%	0.88
30	9.8 mA cm^{-2}	73.2%	8.6%	8.5
40	2.4 mA cm^{-2}	50.5%	34.8%	1.5

References

1. Y. Pan, D. Heryadi, F. Zhou, L. Zhao, G. Lestari, H. Su and Z. Lai, *CrystEngComm*, 2011, **13**, 6937.
2. C. Chen, X. Sun, X. Yan, Y. Wu, H. Liu, Q. Zhu, B. B. A. Bediako and B. Han, *Angew. Chem. Int. Ed.,* 2020, **59**, 11123-11129.
3. S. Gao, Y. Lin, X. Jiao, Y. Sun, Q. Luo, W. Zhang, D. Li, J. Yang and Y. Xie, *Nature*, 2016, **529**, 68-71.
4. X. Kang, L. Li, A. Sheveleva, X. Han, J. Li, L. Liu, F. Tuna, E. J. L. McInnes, B. Han, S. Yang and M. Schroder, *Nat. Commun.,* 2020, **11**, 5464.
5. R. Daiyan, E. C. Lovell, B. Huang, M. Zubair, J. Leverett, Q. Zhang, S. Lim, J. Horlyck, J. Tang, X. Lu, K. Kalantar-Zadeh, J. N. Hart, N. M. Bedford and R. Amal, *Adv. Energy Mater.*, 2020, **10**, 2001381.
6. B. Qin, Y. Li, H. Fu, H. Wang, S. Chen, Z. Liu and F. Peng, *ACS Appl. Mater. Interfaces*, 2018, **10**, 20530-20539.
7. B. Qin, Q. Zhang, Y. H. Li, G. Yang and F. Peng, *ACS Appl. Mater. Interfaces*, 2020, **12**, 30466-30473.
8. I. Hjorth, M. Nord, M. Rønning, J. Yang and D. Chen, *Catal. Today*, 2020, **357**, 311-321.
9. S. Lamaison, D. Wakerley, D. Montero, G. Rousse, D. Taverna, D. Giaume, D. Mercier, J. Blanchard, H. N. Tran, M. Fontecave and V. Mougel, *ChemSusChem*, 2019, **12**, 511-517.
10. M. Beheshti, S. Kakooei, M. C. Ismail and S. Shahrestani, *Electrochim. Acta*, 2020, **341**, 135976.
11. N. Meng, C. Liu, Y. Liu, Y. Yu and B. Zhang, *Angew. Chem. Int. Ed*., 2019, **58**, 18908-18912.
12. H. Guzman, D. Roldan, A. Sacco, M. Castellino, M. Fontana, N. Russo and S. Hernandez, *Nanomaterials (Basel)*, 2021, **11**, 3052.
13. K. Han, P. Ngene and P. de Jongh, *ChemCatChem*, 2021, **13**, 1998-2004.
14. K. Malik, B. M. Rajbongshi and A. Verma, *J. CO_2 Util.*, 2019, **33**, 311-319.
15. C. Ma, X. Zou, A. Li, Z. Gao, L. Luo, S. Shen, J. Zhang, Z. Huang and L. Zhu, *Electrochim. Acta*, 2022, **411**, 140098.
16. P. Li, J. Liu, J. Bi, Q. Zhu, T. Wu, J. Ma, F. Zhang, J. Jia and B. Han, *Green Chem*., 2022, **24**, 1439-1444.
17. J. Young Maeng, J. Hyun Yang, H. Ji Jang, M. Hee Joo, Y. Jun Kim, C. Kyun Rhee and Y. Sohn, *Appl. Surf. Sci.*, 2023, **609**, 155349.